Nuclear Fusion Power Reactor Concept Proposed for Laser-Driven Proton-Boron (HB11) Fusion

I.C. Edmond Turcu

UKRI/STFC Central Laser Facility, Harwell Campus, Didcot, UK

edmond.turcu@stfc.ac.uk

Talk at Int Workshop Proton Boron Fusion 2025, Belgrade
Monday, 8th of Sept 2025

Science and Technology Facilities Council

Content

Science and Technology Facilities Council

First-Wall Life-Time Limitations and Solutions

HiPER technical report

HiPER Building

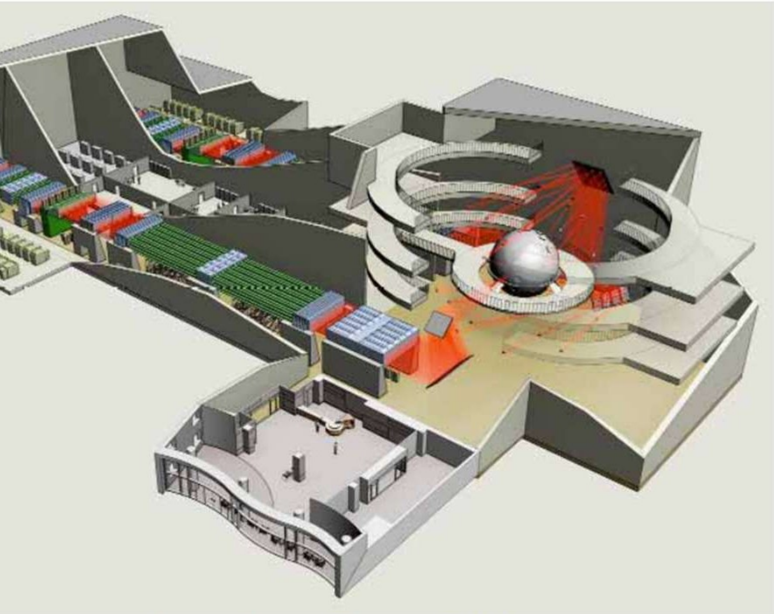

Figure 14.1 Aerial Schematic of HiPER

HiPER Technical Background
nceptual Design Report 2007
ort is available on the HiPER website
iper-laser.org

Science and Technology Facilities Council

- **1 Year from Neutron Radiation Damage** at Full 3GW-Fusion Radiation Power: 400MJ x 6.7Hz
  - Solution: Increase First Wall DISTANCE to Fusion Source: Reduce Neutron Flux Increase Life-Time

- **~Seconds from Ion Radiation Damage** = 20% of Total Fusion Radiation Power for DT
  - Solution: Buffer Gas '**STOPS**' **Ions: Eliminates Damage** see Book ⟶

[2] R. Gonzales-Arrabal, "Materials and Technology for Inertial Fusion Reactors: Lessons Learned from the **HiPER** Project", DDFI-2025 .

[3] R. Gonzalez-Arrabal, A. Rivera, J.M. Perlado, "Limitations for tungsten as plasma facing material in the diverse scenarios of the European inertial confinement fusion facility HiPER: Current status and new approaches", Matter Radiat. Extremes 5, 055201 (2020)

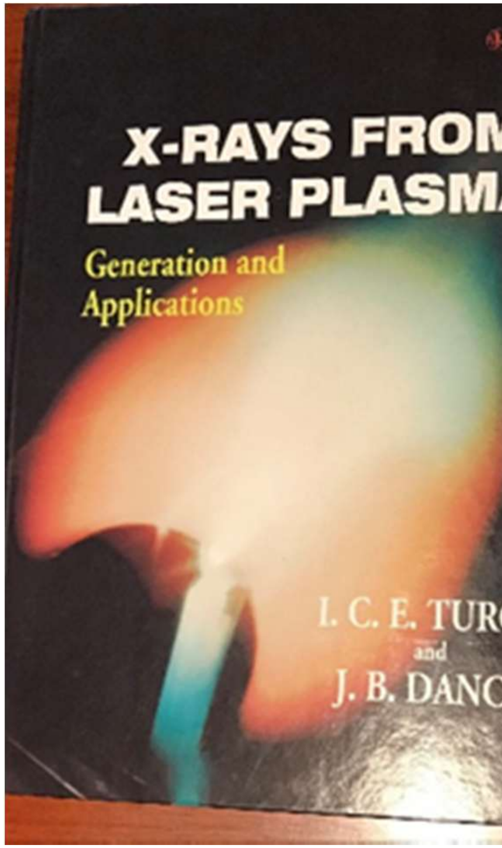

[4] ICE Turcu and Brian
"X-Rays from Laser Plasr
Generation and Applicatio
J Wiley and Sons, 1998

on Reactor Driven by Lasers: No stringent space LIMITATIONS on DIMENSIONS

Plasma/Reactor Chamber: Example for DT Reactor.

First Wall Distance not Limited
mond DDFI-2025 GSI Darmstadt

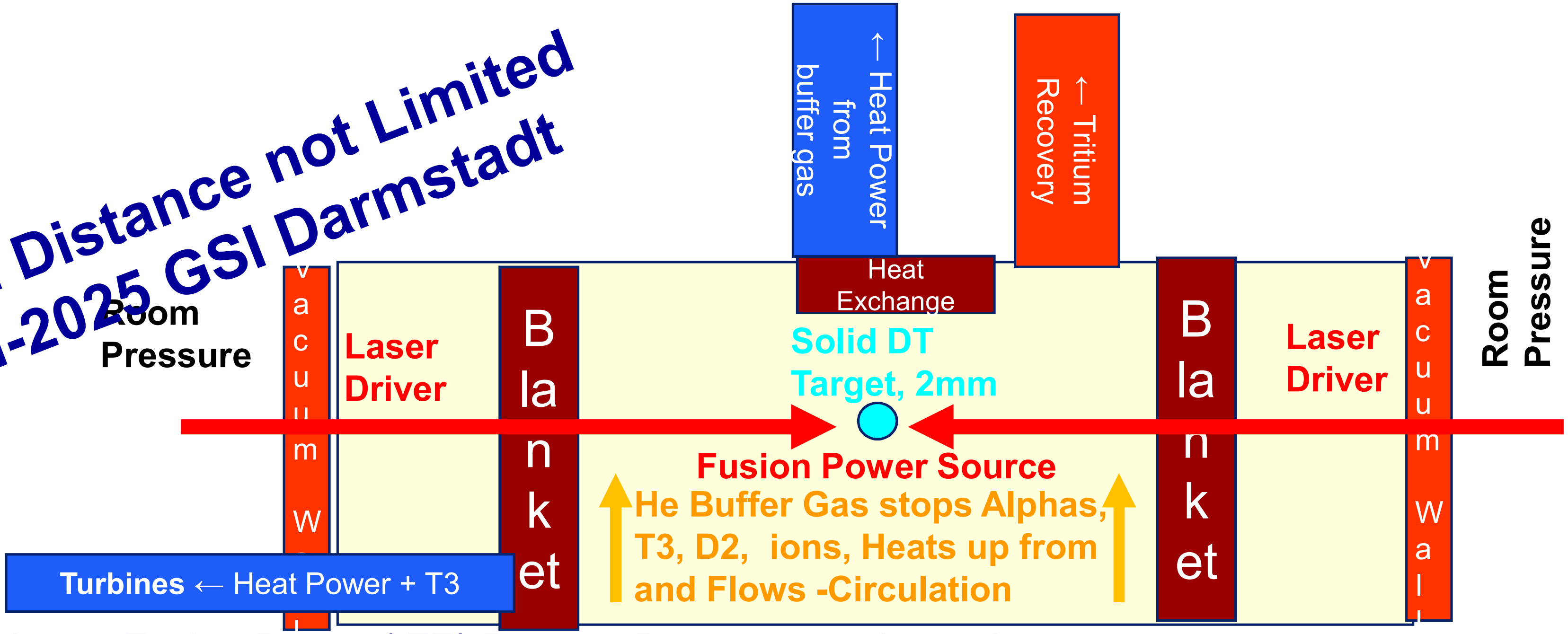

Laser Fusion Power (IFE) Reactor Proposal – schematic

- Small mm-size Solid DT target in Centre of Reactor
- Pulsed Operation – Scale Power by Laser Rep Rate

No stringent space LIMITATIONS on Plasma/Reactor Chamber DIMENSIONS

- Blanket Pannels, not Vacuum-tight convert 80% of P-Fusion + T3
- Blanket panels, and closest mirrors - consumables
- **Vacuum wall separated in space from Blanket.** Permanent wall.

Buffer Gas fills the whole Reactor/'Vacuum' Chamber

- 3MeV Alphas and Ion-debris stopped in Buffer Gas which heats up, converting 20% Fusion-Power to
- Heat exchanger at top of Reactor sends this 20% Power **to Turbines**

aser-IFE Reactor Concept – Vertical Plane Crossection Schematic: Neutron Blanket-Conve
PARATE from Vacuum Wall. Vacuum Wall is External Wall protected from Radiation: Neut
Buffer gas in chamber stops ions/debris and Converts Alpha Power to Heat Power.
uffer gas stiops T3 and D2 – collect in top hot gas container, cooled and separated in T ar

First Wall Distance =20meters
Diamond DDFI-2025 GSI Darmstadt

um and Deuterium~10KeV are
pped in He gas.
nd D collect at top of chamber
l the hot He.
t exchanger extract heat ~20% of
ion Power, 500MW for Hyper.

nd D is separated from He.

0% of 200gT3 Fuel/day burned
5 g T3/day, same of D.
nishing by breeding 75 g T3/day

% of Fuel can be recovered and
led: 125gT3/day.

RGET INJECTION through the COLD
- Bottom of Reactor Chamber

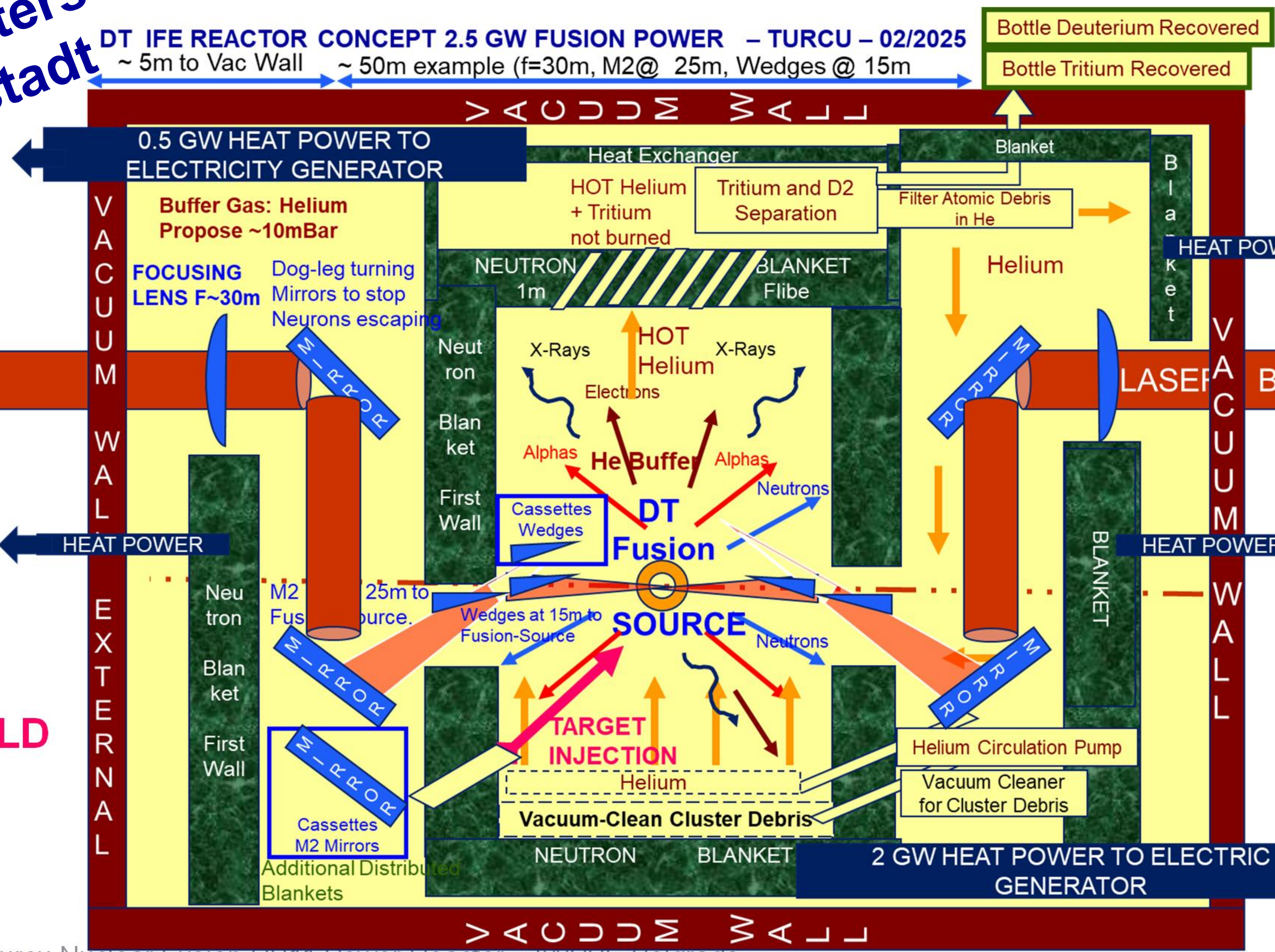

Science and Technology Facilities Council

Extend Concept to Aneutronic Fusion Power Reactors: Ion and X-Ray Radiation instead of Neutron Radiation

usion:

MeV Neutrons 80% Fusion Power: heat First Wall and
ed Heat Power to Electric Generators.
leV Alphas 20% of Fusion Power: Heat Buffer gas, heat
changer, Heat to Electric Generators
% X-rays

fuel	T_i [keV]	$P_{fusion}/P_{Bremsstra}$
$^2_1D-^3_1T$	50	140
$^2_1D-^2_1D$	500	2.9
$^2_1D-^3_2He$	100	5.3
$^3_2He-^3_2He$	1000	0.72
$p^+-^6_3Li$	800	0.21
$p^+-^{11}_5B$	300	0.57

on Boron Fusion and Deuterium-Helium-3 : Preferred tions

leV Alphas 100% of Fusion Power: Heat Buffer gas,
at exchanger, Heat to Electric Generators
JT, Significant Bremsstrahlung emission because of
oron with Z=5. Also part of the Alpha Energy heats
ectrons which generate even more Bremsstrahlung.
ample: 50/50% Alpha-Xray emission – work required:
ray Bremsstrahlung Power Direct Conversion to ectric Power in X-Ray PIN Diodes or 'X-Ray onverter Pannels' : Solar X-Ray-Panels for OUR Artificial X-Ray-Sun

fuel	Z	E_{fus} [MeV]	E_{ch} [MeV]	neutro
$^2_1D-^3_1T$	1	17.6	3.5	
$^2_1D-^2_1D$	1	12.5	4.2	
$^2_1D-^3_2He$	2	18.3	18.3	
$p^+-^{11}_5B$	5	8.7	8.7	≈

Facilities Council

HB11 and DHe3 Fusion Fuels for Aneutronic Fusion Power Reactors:

1 Fuel solid at Room temperature, example:
NH6, Ammonia Borane NOT Cryogenic, non-Toxic
2H6, Di-Borane, LN2 Cryogenic, Toxic
-Ray Bremsstrahlung: Large Fraction
igher Fusion Temperature than DHe3
igher Fusion Crossectionn but over narrow Energy Range
eutron Very Low emission

3 Fuel:
eed to produce He3 for example from DD Beam Fusion
ryogenic
-Ray Bremsstrahlung: Considerable Fraction
eutron Low emission

fuel	T_i [keV]	$P_{fusion}/P_{Bremsstra}$
${}^2_1D-{}^3_1T$	50	140
${}^2_1D-{}^2_1D$	500	2.9
${}^2_1D-{}^3_2He$	100	5.3
${}^3_2He-{}^3_2He$	1000	0.72
$p^+-{}^6_3Li$	800	0.21
$p^+-{}^{11}_5B$	300	0.57

fuel	Z	E_{fus} [MeV]	E_{ch} [MeV]	neutro
${}^2_1D-{}^3_1T$	1	17.6	3.5	
${}^2_1D-{}^2_1D$	1	12.5	4.2	
${}^2_1D-{}^3_2He$	2	18.3	18.3	
$p^+-{}^{11}_5B$	5	8.7	8.7	≈

Science and Technology Facilities Council

ser-IFE Proton-Boron Reactor Concept-example with only two laser beams: Only Residual Neu
adiation. X-Ray 'Solar Pannels' convert X-rays directly to Electricity. Vacuum Wall is External W
Buffer gas in chamber stops ions and Converts Alpha Power to Heat Power.

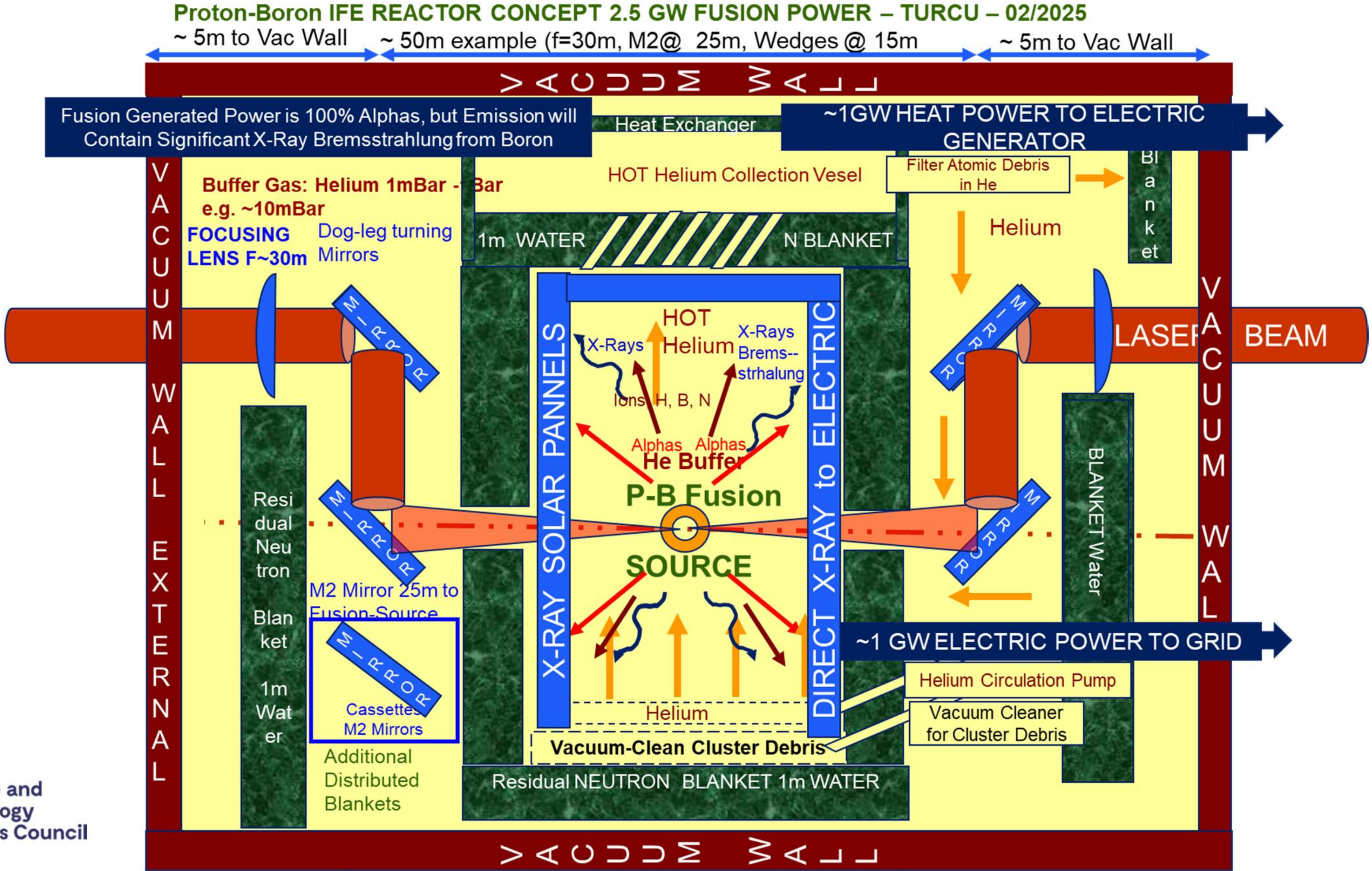

Science and Technology Facilities Council

ffer Gas Stops 3MeV Alphas and Convert their Energy into Heat. Also stops all 'Ionic debr

/ **Alpha Range in He at** 1atmosphre: 1.5 x 10^{-3} cm^2/g [Williamson et al., CEA-R-3042 (1966)].
ange ~ 9cm at 1000mBar Buffer pressure: ρ (He atm) = 1.64x10^{-4} g/cm^2
ange ~ 10m at 10mBar Buffer pressure – assume our IFE Reactor works with 10mBar He buffer.
ange is shorter ~ 1meter if we consider the interaction of $Alpha^{+2}$ with IONIZED He^{+2} Buffer Gas even at 10mBar pres
Snow-Plough Effect" [Marshall L. Ginter and Thomas J. Mcilrath, Debris and VUV emission from a laser-produced plasma", APPLIED PTICS, 5, 885-9 (1988); D. W. Koopman and R. R. Goforth, "Collisional Coupling in Counterstreaming Laser-Produced Plasmas," Phys. uids 17, 1560 (1974)]
means most 3MeV Alphas are stopped within ~ meter Radius of Fusion ce even in 10mBar of He.

Gas Eliminates Debris Damage: experimental proof
fer 1Bar + Flow:100W, 100Hz, laser, >$10^{15}$$W/cm^2$;
/ tape 20um thick **[Turcu, J Wiley 1998],** work at CLF, UK
ontinuous operation as industrial Prototype at JMAR in ego: **0.3Bar, 300W laser, 300Hz, >$10^{15}$$W/cm^2$**
mic Debris eliminated by 'Snow-plough' effect
eraction of plasma ions with He^{+2} Buffer Ions. Cu vapour densates and deposits in the filter of the flow system.
ster Debris are heavy and falls at the bottom of the mber.

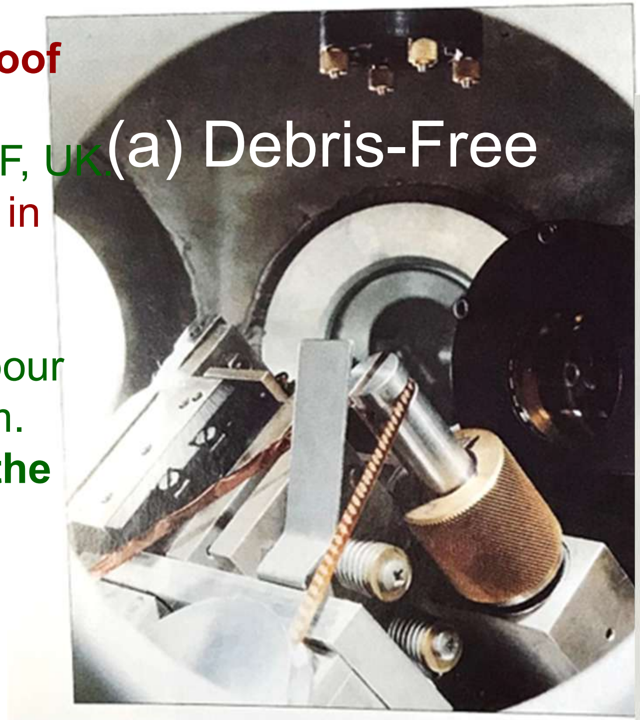

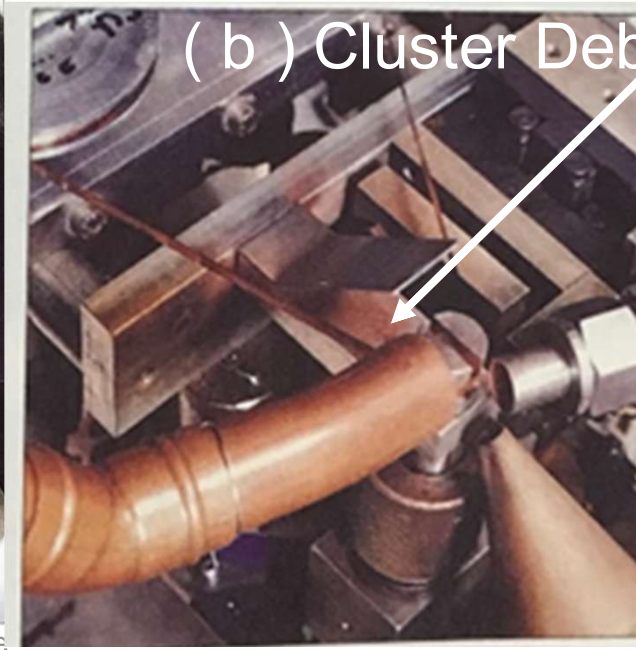

Science and Technology Facilities Council

fer Gas considerations: He Gas Breakdown Intensity >10^{14} -10^{15} W/cm^2 for 25ns UV las 0.25um Laser: LPP X-Ray KeV emission unchanged by He Buffer gas to 1Atm

ffer Pressure and Type and Gas is chosen for the highest
eakdown Threshold. X-Ray Source: No X-ray Loss in Buffer Gas
F: KrF (0.25um) He-1Bar, JMAR YAG (1um) laser, He 0.3Bar

High-Power Laser Plasma X-Ray Source

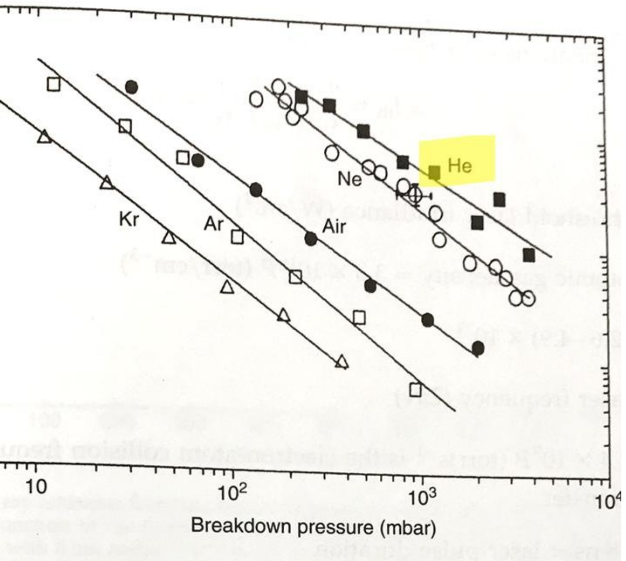

a) also shows that the helium gas breakdown threshold laser is inversely proportional to the gas pressure (P):

$$I_{th} \approx 6.9 \times 10^{15} P(\text{mbar})^{-1}$$

od agreement with an inverse Bremsstrahlung absorption process breakdown. Morgan *et al.* [6] have shown that for short laser pulses,

217

218 X-Rays from Laser Plasmas

in the case of the gas breakdown dominated by inverse Bremsstrahlung absorption, the relationship between I_{th} and P is [7]

$$I_{th} \approx \frac{n_a}{c_i}\left(\frac{\omega}{\nu_{ea}}\right)^2 \frac{1}{\tau_L} \ln(i_B V_F n_a)$$

where

I_{th} = threshold laser irradiance (W/cm^2)

n_a = atomic gas density = $3.3 \times 10^{16} P$ (torr/cm^{-3})

$c_i = (2.6–4.9) \times 10^{23}$

ω = laser frequency ($2\pi\nu$)

$\nu_{ea} = 2.4 \times 10^9 P$ (torr)s^{-1} is the electron-atom collision frequency for momentum transfer

τ_L = 18 ns = laser pulse duration

$i_B = n_e/n_a \approx 10^{-3}$ = degree of ionization required for breakdown initiation

V_F = about 10 μm^3 in the experiment described above

In addition to the breakdown threshold irradiance being inversely proportional the gas pressure, it is also inversely proportional to the laser pulse duration. his implies that when the pulse duration is reduced from 18 ns to, say, 5 ps, the eakdown threshold for helium gas at atmospheric pressure should increase om 5×10^{12} to 1.8×10^{16} W/cm^2. This is higher than the irradiance used for the icosecond KrF laser system (Section 6.2) that generates the plasma source ection 7.8).

High-Power Laser Plasma X-Ray Source

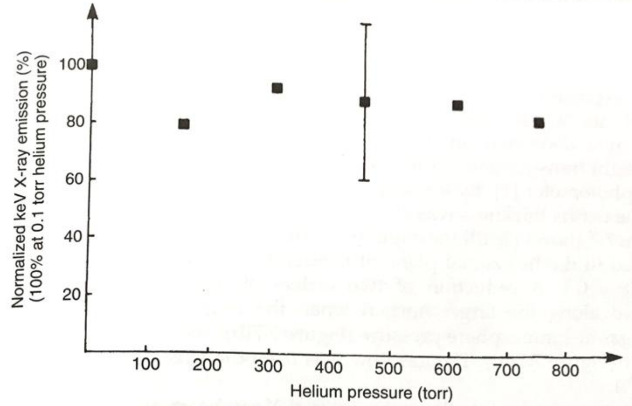

Figure 7.6 X-ray emission from the copper target (Cu L-shell) irradiated by the r system, as a function of the helium pressure in the target chamber. The signal f diode (filtered with 6 μm mylar + 60 nm Al) is compensated for the helium absorp and normalized to the signal recorded when the target chamber is in vacuum estimated shot-to-shot error is shown by the error bar. (Reproduced from Ref. 1)

the paragraph above. This result is important, since it allows a l used in the X-ray chamber. This makes it possible to:

(a) Stop target debris from reaching the lens and the X-ray beam
(b) Increase the X-ray source average power by increasing the r the laser, as the gaseous debris from the target accumulated target can now be removed by flowing helium (Figure 7.2). It a 20 l atm/min cm^2 helium flow rate allowed a repetition rat [2]. When the repetition rate of the '20 ns KrF laser system' (7.4) is increased above this value, the X-ray emission stops a and a 'searchlight effect' appears; i.e. the laser beam propa the target is absorbed and scattered by the atomic debris giving the appearance of a searchlight focused in fog. The e when the helium flow rate is increased.
(c) Use a thin X-ray window in the X-ray beamline, as there difference between the X-ray chamber and the external atmo

.3 Reduction of target debris by the buffer gas

.3.1 *Atomic debris*

The debris reduction obtained by filling the target chamber with compared with operation in a vacuum. The deposition rate of quartz plates placed 77 mm from the plasma source was meas

-I-N Silicon/Ge/Diamond X-Ray Diodes, XRD, Convert LPP X-rays a
JV Radiation to Electric Power, even ≥100keV Bremsstrahlung Photo

RD:
efficiency of 100%
responds to a sensitivity of
7 C/J = e-charge/ gap-Si =
exp-19 C / 3.7eV
Ds can work in pulse mode
P) and in continuous mode
kamaks)
de materials: Si, Ge,
mond, etc.
rmally used as X-ray
tectors with area of mm^2 to
^{2}.
e could build a matrix of
ch diodes to cover full solid
gles around Laser-Fusion
sma.

intensifier, on the phosphor plate by taking an image with a Polaroid or CCD camera. This deflection is proportional to the emission time with respect to a zero-time fiducial. Figure 3.6(b) shows a view of the Kentech [5] re-entrant streak camera, operating in the vacuum of the X-ray chamber with no X-ray window.

3.3 The p-i-n X-Ray Diode

The calibrated detectors used in most of this work are p-i-n silicon semiconductor X-ray diodes (PIN-XRD) manufactured by the Quantrad Corporation [6]. In comparison with vacuum X-ray diodes, the semiconductor X-ray diodes do not require vacuum operation and the sensitivity of the active region does not degrade in time. Thus they provide reliable, calibrated measurements. Their sensitivity is restricted to X-ray photon energies above 0.3 keV, and usually above 1 keV. However, ultra-thin window diodes are manufactured that offer good sensitivity to lower photon energies.

As nearly all the energy of the X-ray photon is used to generate many electron–hole pairs, the sensitivity of the PIN-XRD is some orders of magnitude higher than that of vacuum X-ray diodes. Figure 3.7 is a schematic representation and internal field profile of a semiconductor X-ray detector [7]. The X-ray interaction depicted is the Compton effect, which occurs at medium X-ray energies. In the case of soft X-rays, photoelectrons and Auger electrons are generated in the semiconductor material. The active region, D, of the detector is the intrinsic silicon region. As this type of detector is the main calibrated X-ray

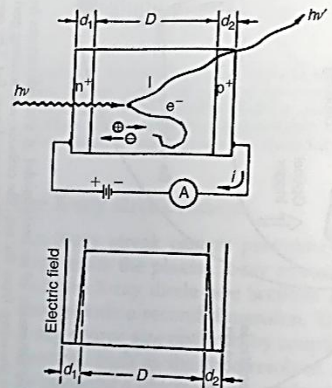

Figure 3.7 Schematic representation and internal field profile of a semiconductor X-ray detector. The X-ray interaction pictured is the Compton effect which occurs at medium X-ray energies. In the case of soft X-rays only electrons are generated (photoelectrons and Auger electrons). (From Ref. 7)

Interaction of Soft X-Rays with Matter: Particle Behaviour

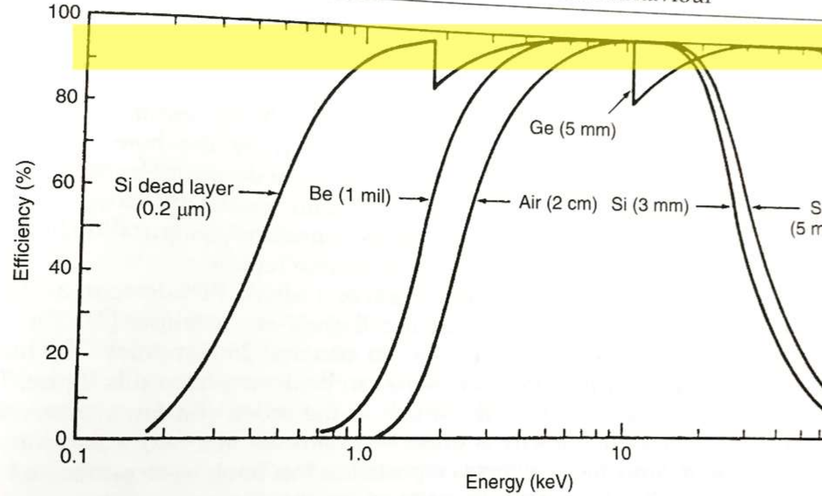

Figure 3.9 Detection efficiency of semiconductor crystals as a function of X-ray photon ene thickness of the dead layer of silicon crystals limits the efficiency at low photon energies; the of the detector crystal limits the detection of high-energy photons; and absorption of b windows and environmental gases, like air, also limit the efficiency at low photon energies. (*X-Ray Data Booklet* [2])

Life-Time of X-Ray-Panel Converter at Large Distance to Fusion Source

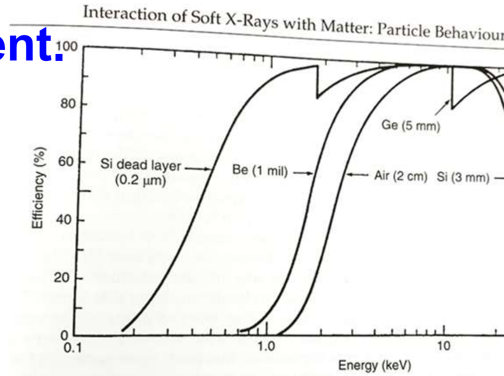

Figure 3.9 Detection efficiency of semiconductor crystals as a function of X-ra
thickness of the dead layer of silicon crystals limits the efficiency at low photon
of the detector crystal limits the detection of high-energy photons; and ab
windows and environmental gases, like air, also limit the efficiency at low phot
X-Ray Data Booklet [2])

RD (X-ray Diodes) convert efficiently X-ray energy directly into electric current.

ime of PIN XRD in GW X-Ray Flux, ~100KeV photons?

because proposed First Wall Distance to Fusion Source is Large

X-Ray Flux on XRD Panel at Large Distance from Fusion Source:
0m, Flux~250 Watt-X-Ray/cm^2
0m, Flux~65 Watt-X-Ray/cm^2

ing measurements of SXUV100 diode
O CHANGE in X-Ray, 100eV, Sensitivity after large dose on
SXUV100 diode: 160 kJ/cm2.
ote XRD with more EUV protection: window of metal-silicide instead of SiO2.
R Korde et. al., Metrologia, 40, S145-S149 (2003); F. Scholtze et al., "Irradiation stability of Silicon
otodiodes for EUV Radiation", Applied Optics, 42, 5621-5626 (2003).
ork on Hardening XRD for Space Missions is Ongoing.

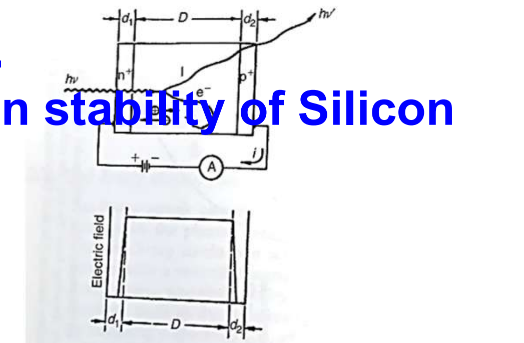

Figure 3.7 Schematic representation and internal field profile of a semic
The X-ray interaction pictured is the Compton effect which occurs at me
the case of soft X-rays only electrons are generated (photoelectrons and
Ref. 7)

Science and Technology Facilities Council

Conclusions

1. HiPER Laser-Driven Fusion Reactor as Benchmark
2. First Wall Life Limits for DT Fusion Power Reactor DDFI2025
3. First Wall Concept: Insert Buffer Gas: 'Ion damage elimination' and 'working gas' DDFI2025
4. 50m IFE Reactor 'Diameter': reduce Neutron flux and increase Wall Lifetime, DDFI-2025
5. EXTEND Reactor Concept to Aneutronic Fusion: HB11 and DHe3
6. Buffer Gas Converts the Fusion Ion Radiation Power into Thermal Power
7. Replace Neutron Radiation Convertor Wall with X-Ray Radiation Power Converter Panels
8. HB11 and DHe3 Aneutronic Fusion Fuels comparison

Science and Technology Facilities Council

Acknowledgements

ICET thanks his colleagues in the Plasma Physics Group and the UPLiFT Group: Alex Robinson, Robbie Scott, Tony Bell, Raoul Trines, Calum Freeman, Arun Nutter, Robert Paddock and Divya Tank, for discussions in the two UPLiFT seminars where he presented the new proposed solution/geometry of the Fusion Reactor Wall. Thanks also to Martin Tolley for discussions on HiPER Reactor.

PROBONO CA21128

Science and Technology Facilities Council


хвала !
Hvala vam
Thank You!